Journal of Membrane Science 367 (2011) 197–203

Contents lists available at ScienceDirect

Journal of Membrane Science

journal homepage: www.elsevier.com/locate/memsci

CO_2–CH_4 permeation in high zeolite 4A loading mixed matrix membranes

Ryan T. Adams, Jong Suk Lee, Tae-Hyun Bae, Jason K. Ward, J.R. Johnson, Christopher W. Jones, Sankar Nair, William J. Koros*

Georgia Institute of Technology, School of Chemical & Biomolecular Engineering, 311 Ferst Drive, Atlanta, GA 30332, USA

ARTICLE INFO

Article history:
Received 29 July 2010
Received in revised form 21 October 2010
Accepted 28 October 2010
Available online 3 November 2010

Keywords:
Mixed matrix membrane
Natural gas
Mixed gas
High loading
Gas separation

ABSTRACT

Mixed matrix membranes (MMMs) with low particle loadings have been shown to improve the properties of pure polymers for many gas separations. Comparatively few reports have been made for high particle loading (≥50 vol.%) MMMs. In this work, CO_2–CH_4 feeds were used to study the potential of 50 vol.% zeolite 4A-poly(vinyl acetate) (PVAc) MMMs for natural gas separations. A low CO_2 partial pressure mixed feed probed MMM performance below the plasticization pressure of PVAc and a high CO_2 partial pressure mixed feed probed MMM performance at industrially relevant conditions above the plasticization pressure.

Under both mixed feed conditions at 35 °C, substantial improvements in overall separation performance were observed. At low CO_2 partial pressures, CO_2 permeability roughly doubled with a nearly 50% increase in selectivity versus pure PVAc under the same conditions. For the high CO_2 partial pressure feed, CO_2 permeability remained effectively unchanged with a 63% increase in selectivity versus pure PVAc. Surprisingly, the performance of these PVAc based MMMs approached the properties of current "upper bound" polymers. Overall, this work shows that significantly improved performance MMMs can be made with traditional techniques from a low cost, low performance polymer without costly adhesion promoters.

Published by Elsevier B.V.

1. Introduction

Dispersing filler particles in polymeric matrices is an increasingly popular method for improving pure polymeric gas transport properties [1–19]. Mixed matrix membranes (MMMs) typically consist of zeolite particles dispersed in polymers with the goal of increasing permeabilities and selectivities of desired components over those of undesired components. MMMs combine the ease of processing polymer membranes with the superior transport properties of zeolitic (and other filler) materials, ideally resulting in membranes with properties that exceed gas pair "upper-bounds" [1,20–22]. Models predict that transport enhancements increase rapidly at high filler loadings [23,24]. While there have been many reports of low filler loading (≤40 vol.%) MMMs showing improved transport properties over their pure polymeric matrices [1–16,19,22,25–27], only a few reports of high particle loading (≥50 vol.%) MMMs have been published [2,3,5,11,12].

Most MMM studies report only low pressure, pure gas permeation data. While low pressure, pure gas permeation experiments can be useful for characterizing new membrane materials, real feeds are complex mixtures and are often at high pressures. Mixed feed permeation properties can substantially deviate from pure gas data due to plasticization, competitive sorption, and many other complicating effects [28,29]. Natural gas sweetening (i.e. removal of acid gases like carbon dioxide and hydrogen sulfide from methane) is among the most important target feeds for membrane separations. Moreover, economic analyses show that natural gas wells with high carbon dioxide concentrations (>20% CO_2) are especially attractive targets for membrane based separations [28,30–33]. Such natural gas sources are processed at total feed pressures as high as 900 psi or more [33]. These considerations encourage testing MMMs under high pressure, simulated natural gas feeds.

In this work, high zeolite 4A loading (50 vol.%) MMMs were made using poly(vinyl acetate) (PVAc) as the matrix polymer. PVAc is well known to be a model polymer for MMM studies due to its flexibility and adhesive properties [1,22,34]. Also, PVAc is known to be sensitive to plasticization-induced loss in selectivity; however, stabilization of chain segments in the vicinity of solids may reduce this sensitivity. PVAc was, therefore, selected as the polymer matrix for this study. Two 50 vol.% zeolite 4A-PVAc MMMs were made from in-house synthesized zeolite 4A via solution processing. These MMMs were tested under two simulated natural gas feeds (dry CO_2–CH_4 at 35 °C): 1) a low case and 2) a high p_{CO_2} case. The individual component permeabilities and CO_2–CH_4 selectivities are reported and compared to pure PVAc values under the same conditions.

* Corresponding author. Tel.: +1 4043852845; fax: +1 4043852683.
E-mail address: wjk@chbe.gatech.edu (W.J. Koros).

0376-7388/$ – see front matter. Published by Elsevier B.V.
doi:10.1016/j.memsci.2010.10.059

2. Theory and background

2.1. Gas permeability in dense membrane materials

The phenomenological definition of gas permeability, P, of a penetrant, i, in dense membranes (such as those studied in this work) is the penetrant partial pressure differential (Δp_i) and membrane thickness (l) normalized flux (N_i) as given in Eq. (1):

$$P_i = \frac{N_i \times l}{\Delta p_i} \quad (1)$$

The underlying basis for gas permeability through dense membranes is the solution-diffusion mechanism where the gases first sorb at the membrane surface from a high activity feed, then diffuse across the membrane thickness along a chemical potential gradient, and finally desorb into a lower activity permeate.

Eq. (1) can be rearranged using Fick's 1st law to give the simple thermo-kinetic expression for permeability shown in Eq. (2):

$$P_i = D_i \times S_i \quad (2)$$

In Eq. (2), S_i and D_i, are the solubility and diffusivity coefficients of penetrant, i, respectively. While permeability defines the productivity of a membrane material, the efficiency of a membrane separation is often expressed as the ratio of the permeabilities of 2 gases known as permselectivity, α, as shown in Eq. (3).

$$\alpha_{i/j} = \frac{P_i}{P_j} \quad (3)$$

The subscripts i and j represent the faster and slower permeating species, respectively, so that permselectivities are always greater than one.

2.2. Gas diffusivity and solubility in membrane materials

For glassy polymers, the diffusivity term in Eq. (2), D_i, is an effective, average diffusivity [35–37]. Barrer showed that there are up to 4 relevant diffusivity terms for glassy polymers involving: 1) diffusional jumps between Henry's sites; 2) diffusional jumps between Langmuir sites, 3) Henry's to Langmuir diffusional jumps, and 4) Langmuir to Henry's diffusional jumps [37]. Diffusion in zeolites is also complex—in fact, it has recently been stated that "accurate determination of gas diffusion coefficients in zeolites will continue to be a problem in the coming decades [38]." Since gas diffusivities in the component materials of a MMM are known to be complex, it clearly follows that gas diffusivities in MMMs are similarly complex. In fact, extending Barrer's 4 components of diffusion in glassy polymers to glassy polymer-zeolite MMMs, with the inclusion of well known interfacial zones of influence around particles [34,39,40], results in no less than 12 potentially relevant diffusivity terms.

The solubility coefficient, S_i, is simply the equilibrium sorbed concentration of a gas in the membrane material divided by the external partial pressure of the gas. Gas solubility coefficients in polymers depend strongly on the proximity to the glass transition temperature, T_g, of the polymers. Rubbery polymers (i.e. polymers above T_g) obey a simple Henry's law solubility response while glassy polymers (i.e. polymers below T_g) exhibit a dual-mode sorption response. This dual-mode response is: 1) a Henry's law response and 2) a Langmuir response caused by excess free volume packets that act as fixed sorption sites. The rigid structures of zeolites result in strictly Langmuir-type sorption responses as described in Eq. (4).

$$C_i = \frac{C'_{Hi} \times b_i \times p_i}{1 + \sum b_j \times p_j} \quad (4)$$

The terms C_i, C'_{Hi}, b_i, and p_i are the sorbed concentration (cc_{STP} gas sorbed/cc zeolite 4A), the Langmuir saturation constant, the Langmuir affinity parameter, and the external partial pressure of component, i, respectively. The term in the summation accounts for competitive sorption on the fixed Langmuir sites in a zeolite where the subscript, j, accounts for all components in the sorbing gas mixture. While modeling diffusivities in a real MMM is complex, gas solubility analysis is much simpler and has been shown to be arithmetic mean of the gas solubilities of each phase [41].

2.3. Computing dispersed phase loading in MMMs

Lack of clarity in the MMM literature regarding dispersed phase loadings complicates understanding MMM transport property enhancements. MMM transport models are typically functions of particle volume loadings; however, many reports of MMM properties describe particle loadings in wt.% or simply %. While accurately determining the appropriate particle density for converting from weight loading to volume loading takes some effort, MMM studies should address this issue. In this work, an "ion-containing" framework density was used for the zeolite 4A density. This value was calculated by summing up the dry unit cell molecular mass of zeolite 4A (including Na^+) and dividing through by the unit cell volume as described by Breck [42]. Framework densities of molecular sieves should be used in MMM studies since it is assumed the matrix polymer is totally excluded from the internal pores of the molecular sieves.

The "ion-containing" framework density of zeolite 4A is 1.52 g/cc [42], and Sigma–Aldrich reports 1.191 g/cc as the density for PVAc. These values were used to compute the mass loading of zeolite 4A in PVAc required to produce MMMs with 50 vol.% 4A loadings in PVAc assuming additivity of volume. Eq. (5) describes the relationship between volume loadings and component masses in MMMs.

$$\varphi = \frac{v_{filler}}{v_{filler} + v_{matrix}} = \frac{m_{filler}/\rho_{filler}}{(m_{filler}/\rho_{filler}) + (m_{matrix}/\rho_{matrix})} \quad (5)$$

In Eq. (5), φ is the filler volume fraction of the MMM, v is the volume, m is the mass, ρ is the density, and the subscripts distinguish between the filler and matrix phase of the MMM (usually a dispersed zeolite phase and a continuous polymer phase, respectively). Using the densities of zeolite 4A and PVAc, and solving Eq. (5) for 50 vol.% loading of zeolite 4A in PVAc, the required mass loading of zeolite 4A is ~56 wt.%.

3. Experimental

3.1. Materials

PVAc (nominal MW = 500 kDa) was purchased from Sigma–Aldrich (Milwaukee, WI). Anhydrous toluene was also purchased from Sigma–Aldrich (Milwaukee, WI) and used without further purification. Zeolite 4A, 0.5–1.5 μm average size was synthesized by our group. The high quality of the zeolite 4A was confirmed by XRD, elemental analysis, cryogenic N_2 physisorption, and pressure decay gas sorption at 35 °C.

3.2. Dense film preparation

Pure PVAc dense film membranes were made from PVAc-toluene solutions. First, ~7 g PVAc beads were dried in 100 °C vacuum for 24 h in a 40 mL glass vial. After cooling to room temperature, the vial was removed from the vacuum oven and the requisite amount of toluene to create a 25 wt.% PVAc-toluene solution was added to the vial (note that the PVAc beads lost a negligible amount of mass upon vacuum drying). The PVAc beads–toluene mixture

was allowed to homogenize on a coaxial roller for several days before use. Dense PVAc membranes were prepared by pouring a small portion of the stock solution on a solid Teflon® plate and casting with a 10 mil casting knife in a dry N_2 purged and backfilled glove bag. Approximately 20 mL of toluene was poured into a Petri dish 1 h before casting and allowed to evaporate in the glove bag to decrease the rate of solvent evaporation from the dense film. Eighteen to twenty four hours later, the pure PVAc film adhered to the Teflon® plate was transferred to a vacuum oven for total toluene evaporation at 200 °C for 24–36 h. It was found by trial-and-error that a slow approach to 200 °C resulted in less bubble formation in the films. We hypothesize that the imperfect surface of the Teflon® plate traps air beneath the films which can create air bubbles. Upon heating and pulling vacuum these trapped air packets grow. By ramping up the temperature slowly, the trapped air has more time to permeate through the film thereby minimizing bubble formation. After cooling to room temperature under vacuum the pure PVAc samples were prepared for permeation testing as described elsewhere [43].

Preparation of mixed matrix membranes was considerably more complex. Two to four grams of calcined zeolite 4A were placed in a 100 mL open-topped, round bottom glass reactor and activated for 24–36 h in a 200 °C vacuum oven. After cooling to room temperature, the dry zeolite 4A was quickly weighed (note the calcined zeolite 4A lost ~20% of its mass after vacuum activation at 200 °C) before adding 60–80 mL of anhydrous toluene to the 4A. The 4A-toluene mixture (glass reactor submerged in an ice bath) was then homogenized with 5, 60 s bursts from a 1000 W ultrasonic horn with 30–45 s of vigorous magnetic stir bar mixing in between ultrasonic bursts (note the stir bar was weighed prior to beginning the experiment). Immediately following the final ultrasonic burst, 20 wt.% of the total amount of PVAc required was added from a 25 wt.% PVAc-toluene solution while mixing vigorously with a magnetic stir bar in order to stabilize (or "prime") the 4A-toluene dispersion via PVAc adsorption on the 4A particles [40]. After 5 min of vigorous mixing, the PVAc primed, 4A-toluene dispersion was transferred to a clean, pre-weighed, one-neck, round-bottomed evaporation flask. The total mass of the flask, stir bar, and primed solution was then recorded. Vigorous magnetic stir bar mixing continued for 2 h under a low flow dry N_2 purge before the adding the remainder of the required PVAc was added from the same 25 wt.% PVAc-toluene stock solution previously described.

The resulting solution had a very low viscosity (not measured, visually observed) due to the large amount of toluene required to adequately disperse the 4A particles. In order to knife cast a homogenous MMM dense film that properly wets the Teflon® casting plate, a substantial amount of toluene had to be removed to increase the solution viscosity. A low flow rate (barely detectable with an oil bubbler), dry N_2 purge was used to evaporate toluene to the desired concentration. The low flow rate minimized film formation at the solution-N_2 interface so that the solution remained homogenous. Through trial-and-error, a toluene concentration of $\leq$64 wt.% was found to be optimal for defect-free, 50 vol.% 4A-PVAc MMM formation. Casting solutions with toluene concentrations >64 wt.% resulted in MMMs with poor morphologies (i.e. with void defects). Once the desired toluene concentration was achieved, the N_2 flow was stopped, the one neck flask was sealed with a rubber stopper, and the casting solution was placed on a slow coaxial roller as a final homogenization step (i.e. to reincorporate small amounts of material left on the vial walls during toluene evaporation). The final casting solution was then transferred to clean, 8 mL glass vials and placed on a coaxial roller for a few days before casting. Casting of MMM solutions proceeded similarly to that of the pure PVAc samples. The primary difference was that the cast film remained in the glove bag for an additional day in an effort to reduce the rate of toluene evaporation, and hence, to minimize stress accumulation [40,44,45].

3.3. Permeation testing

Upon cooling dense film samples to room temperature under vacuum, the Teflon® plates were removed and the samples were peeled off the plates with the help of a razor blade. Circular samples (~3/4 inch diameter) were cut from the samples (away from the edges). These samples were formed into "sandwich"-type masks as described in detail elsewhere [43]. These masks were then adhered to the downstream face of the permeation cell with aluminum duct tape and a ring of epoxy was applied to the mask-film edge to prevent gas bypass through the aluminum foil tape adhesive during the long, high pressure CO_2 permeation experiments to follow. Vacuum was then applied to the downstream face of the membrane only while the epoxy on the upstream face was allowed to cure for 24 h in a stagnant, dry N_2 upstream just above atmospheric pressure.

After the epoxy cured, vacuum was pulled on both the upstream and downstream volumes of the permeation system for at least 4 days prior to gas permeation testing. Leak tests were performed on the downstream volume of the permeation system every day before permeation testing began to ensure a constant leak rate was achieved. Note that leak rates never exceeded 0.26% of the total permeate flow rate (or 1.7% of the slow gas, i.e. methane, permeate flow rate).

For both pure PVAc and 50 vol.% 4A-PVAc MMM samples, 2 mixed CO_2–CH_4 permeation feeds were tested at 35 °C: 1) a low p_{CO_2} case where a 10% CO_2-balance CH_4 feed was permeated at 40 psia total pressure and 2) a high p_{CO_2} case where a 50:50 CO_2–CH_4 feed was permeated at 440 psia. Note that the low p_{CO_2} case yielded data below the plasticization pressure, p_{plast}, of pure PVAc, which is indicated by an increasing CO_2 permeability with increasing CO_2 feed pressure. The high p_{CO_2} case was well above p_{plast}. The low p_{CO_2} case was always done first to avoid the potential complications of polymer matrix conditioning by high pressures of CO_2. To prevent concentration polarization, a retentate flow was established on the upstream during mixed feed testing. The ratio of total permeate flow to retentate flow never exceeded 0.002%.

The downstream pressure rise was monitored throughout the permeation experiments. Mixed gas data sampling via gas chromatography did not begin until steady-state permeation was firmly established as witnessed by the time lag method and analysis of the derivative of downstream pressure versus time. The approach to steady state permeation for the MMM samples was extremely slow due to the presence of "mass sinks", i.e. the zeolite 4A particles. This effect is well documented in the literature and is often called immobilizing sorption [17,18,22,46,47]. A full day was required before the high loading 4A MMMs reached steady state permeation, and permeation was allowed to proceed for 2–3 additional days to ensure the samples were stable and maintained the same steady state flow over time before GC sampling. GC samples were taken several times a day for at least 3 more days in order to show sample stability and to generate statistically significant data. Note that pure PVAc mixed gas testing proceeded more rapidly due to its faster approach to steady state permeation; however, GC data was still taken over several days to ensure sample stability. In between testing the low and high p_{CO_2} feeds, vacuum was pulled on the entire permeation system for at least 9 days to fully degas the masking material and dense film sample (degassing progress was monitored by daily leak tests as described earlier for initial sample loading).

3.4. Pressure decay gas sorption on zeolite 4A

Pure gas pressure decay sorption experiments were used to confirm quality of the zeolite 4A. Pressure decay sorption procedures

Table 1
Elemental analysis of zeolite 4A.

Sample	Wt.% oxygen EDS/ICP	Wt.% sodium EDS/ICP	Wt.% aluminum EDS/ICP	Wt.% silicon EDS/ICP
In-house 4A	45.35/na	13.23/11.93	18.41/17.50	23.01/27.64
Literature 4A	45.05	16.18	18.99	19.77

and powder sample preparation are described well in the literature [35,48]. Note that zeolite 4A sorption samples were activated under the same conditions used for MMM preparation as described in Section 3.2. CH_4 isotherms were generated first, followed by CO_2 isotherms at 35 °C.

3.5. Additional zeolite 4A and MMM characterization

Cryogenic N_2 physisorption, X-ray diffraction (XRD), and elemental analysis by inductively coupled plasma (ICP) mass spectrometry and energy dispersive spectroscopy (EDS) were also used to confirm the quality of the synthesized zeolite 4A. From the cryogenic N_2 physisorption experiments the BET surface area is reported. The XRD pattern and composition of the zeolite 4A was compared to those in the literature.

Cross-sectional images of 50 vol.% zeolite 4A-PVAc MMM samples were taken with a scanning electron microscope (SEM). The SEMs were scrutinized to confirm homogenous dispersion of particles and the absence of 4A-PVAc interfacial voids.

4. Results and discussion

4.1. Pure zeolite 4A

Calcined zeolite 4A crystals were prepared using a hydrothermal method that utilized tetramethyl ammonium hydroxide as a structure directing agent. The details of synthesis are omitted for brevity, but a variety of characterization experiments were used to confirm successful zeolite 4A preparation.

ICP mass spectrometry was done by Columbia Analytical Services (Tucson, AZ) to determine the silicon, aluminum, and sodium content of the zeolite 4A. Oxygen content was determined by EDS. Table 1 summarizes the elemental analyses results and compares to the theoretical composition of zeolite 4A. Oxygen content as measured by EDS shows that the zeolite 4A used matches well with theoretical oxygen content. ICP shows that the zeolite 4A is slightly silicon-rich and slightly deficient in aluminum and sodium. Overall the elemental analysis is consistent with a small excess of silicon in the framework (and therefore less aluminum and less sodium needed to balance the charges in the crystals)—this is a well documented phenomenon for LTA zeolites [42].

XRD measurements were made to confirm a crystalline zeolite 4A sample with the correct diffractogram. Fig. 1 shows the diffractogram of the zeolite 4A used in this work plotted with known literature values [49]. It is shown that the synthesized zeolite 4A bears the correct diffraction pattern. Cryogenic nitrogen physisorption experiments were used to determine the BET surface area of the prepared zeolite 4A. A BET surface area of $369.49 \pm 7.11\ m^2/g$ was measured. The composition from the elemental analyses, the XRD pattern, and the fairly high specific BET surface area strongly suggest the successful synthesis of zeolite 4A.

Finally, pure CO_2 and CH_4 pressure decay gas sorption experiments were done on pure zeolite 4A vacuum activated at 200 °C. Figs. 2 and 3 show the CH_4 and CO_2 isotherms (35 °C) of the zeolite 4A used in this work. Langmuir parameters are reported in Table 2. The isotherms and Langmuir parameters match well with those in the literature further confirming the high quality of the zeolite 4A [41].

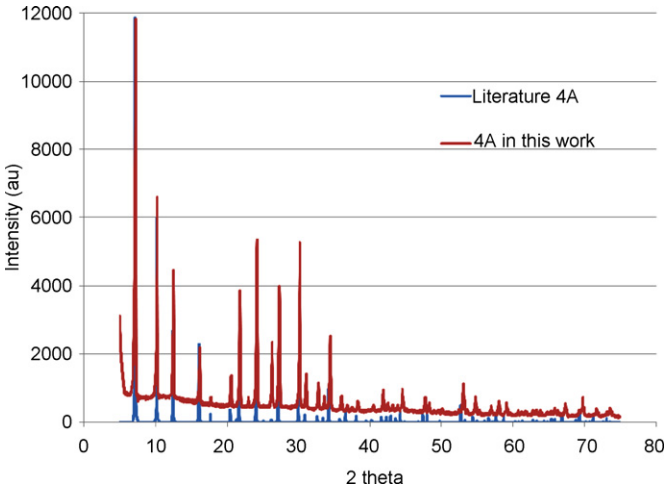

Fig. 1. X-ray diffractograms of in-house synthesized and literature reported zeolite 4A.

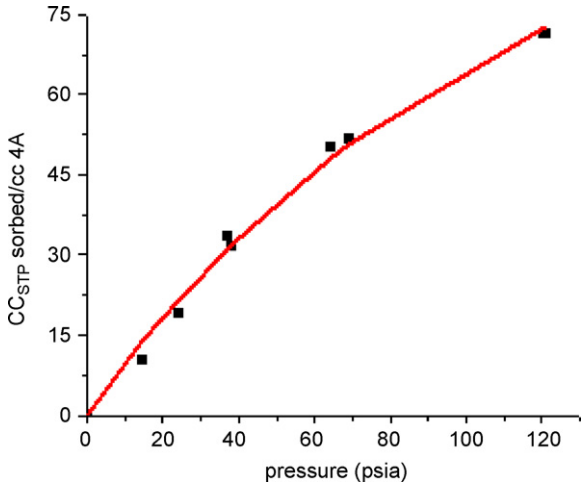

Fig. 2. Methane sorption isotherm (35 °C) of zeolite 4A.

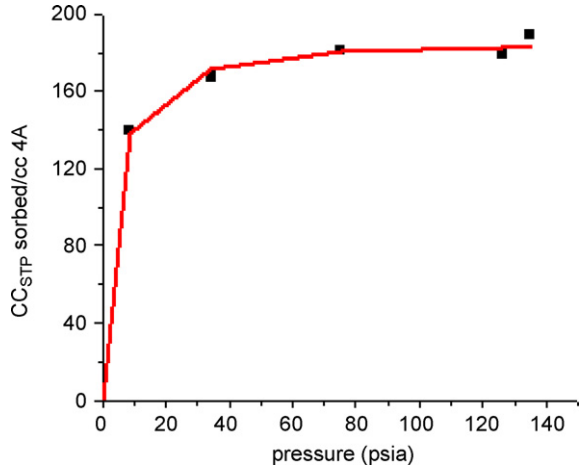

Fig. 3. Carbon dioxide sorption isotherm (35 °C) of zeolite 4A.

Table 2
Langmuir parameters for zeolite 4A.

	C'_{Hi} (cc_{STP}/cc)	b_i ($psia^{-1}$)
CH_4	177.3 ± 27.0	0.0058 ± 0.0013
CO_2	187.6 ± 2.8	0.32 ± 0.045

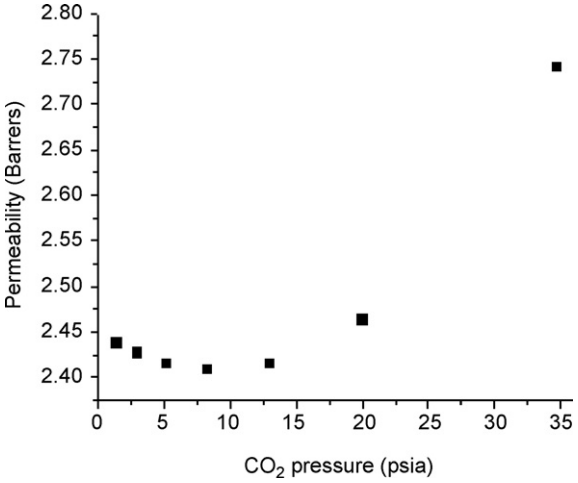

Fig. 4. CO_2 permeation isotherm of PVAc. Plasticization at ~10 psia (minimum of isotherm).

4.2. Pure PVAc

Fig. 4 shows the CO_2 permeation isotherm of PVAc at 35 °C. The minimum at ~10 psia is taken as p_{plast} for CO_2 in PVAc. From Fig. 4 it is shown that the low p_{CO_2} mixed feed permeation case is below p_{plast} whereas the high p_{CO_2} case is well beyond p_{plast}. The shape of the isotherm confirms that PVAc is in the glassy state at 35 °C. Differential scanning calorimetry gives a glass transition temperature, T_g, of 43.5 for the PVAc used in this work.

Table 3 summarizes the mixed feed permeation properties of pure PVAc for both the low (4 psia) and high (220 psia) p_{CO_2} cases at total pressures of 40 and 440 psia, respectively. The effect of plasticization is clearly evident by the drastic 5.3x increase in P_{CO_2} along with 25% reduction in permselectivity.

4.3. 50 vol.% zeolite 4A-PVAc MMM permeation properties

The 50 vol.% zeolite 4A-PVAc MMMs studied in this work had CO_2–CH_4 permeation properties vastly superior to those of pure PVAc under the same feed conditions. Fig. 5 is an SEM showing the cross-section of a high zeolite 4A loading MMM. Homogenous dispersion of particles and the absence of agglomeration are clearly shown. Fig. 6 shows a zoomed in SEM displaying good 4A-PVAc interfacial adhesion. The averaged individual component permeabilities and the CO_2/CH_4 permselectivities for the low p_{CO_2} mixed feed case of 2 separate MMM samples are reported in Table 4. CO_2 permeability more than doubled and permselectivity increased by nearly 50% versus pure PVAc as shown in Table 4 with enhancement factors, Ψ_i. Ψ is simply a ratio of MMM property to the corresponding pure PVAc property, and i represents CO_2 permeability, CH_4 permeability, or CO_2–CH_4 selectivity.

Under the high p_{CO_2} mixed feed, MMM transport enhancements were also impressive (see Table 4). Although the increase in CO_2 permeability is marginal, permselectivity increased by 63%. The lack of significant CO_2 permeability enhancement for the high

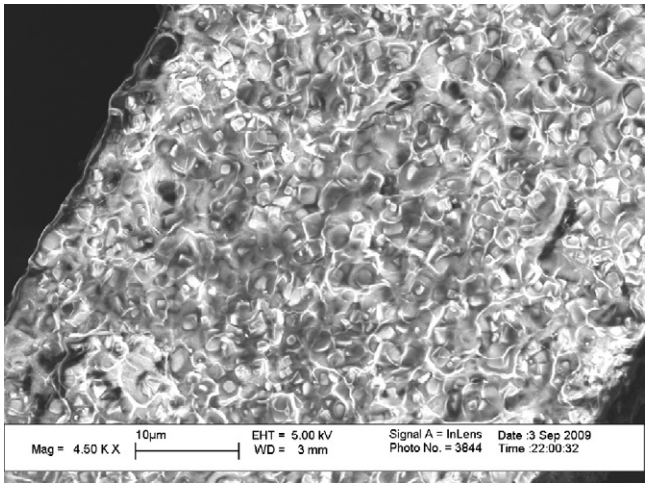

Fig. 5. SEM of a 50 vol.% zeolite 4A-PVAc MMM overall cross-section.

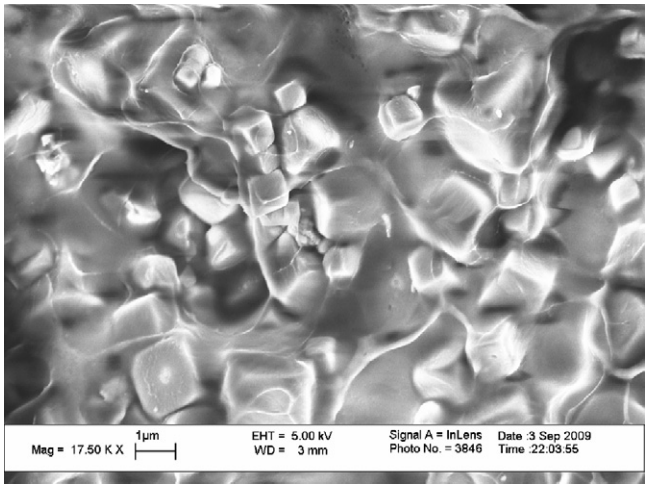

Fig. 6. SEM of a 50 vol.% zeolite 4A-PVAc MMM zoomed in cross-section.

Table 3
Mixed feed permeation summary for pure PVAc samples. Errors are ±1 standard deviation from 2 samples.

	P_{CO_2} (Barrers)	P_{CH_4} (Barrers)	α_{CO_2/CH_4}
Low pressure case (10% mol CO_2, 40 psia)	2.15 ± 0.01	0.064 ± 0.001	33.5 ± 0.4
High pressure case (50% mol CO_2, 440 psia)	11.4 ± 0.1	0.457 ± 0.008	25.0 ± 0.3

Table 4
Low and high pressure mixed feed case MMM data are shown along with corresponding MMM enhancement factors, Ψ_i = MMM/PVAc, where i is CO_2 permeability, CH_4 permeability, or mixed gas selectivity. Errors are ±1 standard deviation from 2 samples.

	P_{CO_2} (Barrers)	Ψp_{CO_2}	P_{CH_4} (Barrers)	Ψp_{CH_4}	α_{CO_2/CH_4}	Ψ_{CO_2/CH_4}
Low p_{CO_2} case	4.33 ± 0.67	2.01	0.088 ± 0.013	1.36	49.4 ± 0.5	1.47
High p_{CO_2} case	11.5 ± 1.2	1.01	0.284 ± 0.037	0.621	40.6 ± 1.8	1.63

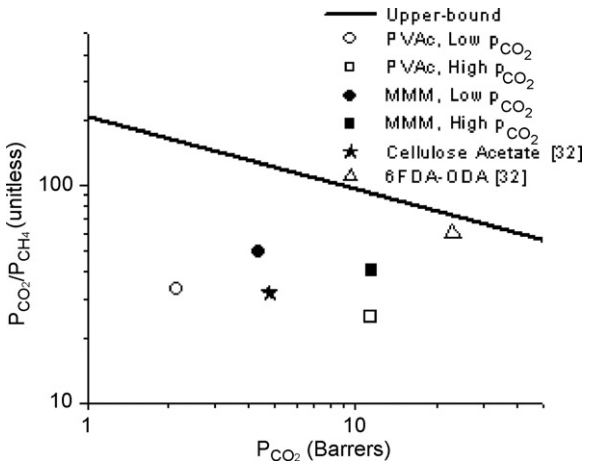

Fig. 7. MMM permeation properties on current CO_2–CH_4 upper-bound [20].

p_{CO_2} case is likely due to Langmuir sorption saturation in the zeolite 4A crystals (as described in Eq. (4)) which results in lower gas solubilities, and hence permeabilities. Use of Eq. (4) and the Langmuir parameters in Table 2 show that solubility selectivity in zeolite 4A remains the same under both feed conditions at $S_{CO_2}/S_{CH_4} = 59.7$. Assuming that diffusion selectivity in the dispersed 4A particles remains unchanged for each feed, it follows that the larger selectivity enhancement factor (Ψ_{CO_2/CH_4}) for the MMM in the high pressure versus the low pressure mixed feed is the result of lower separation efficiency of pure PVAc above the plasticization pressure. In other words, the change in pure PVAc permeation properties upon plasticization results in altered filler-matrix matching that does not favor significant enhancement of CO_2 permeability although it does substantially suppress methane permeability due to competitive sorption in the zeolite [1,50].

Fig. 7 highlights the extremely desirable mixed CO_2–CH_4 transport enhancement trends for high zeolite 4A loading PVAc MMMs by plotting the CO_2 permeabilities and CO_2/CH_4 permselectivities on Robeson's most current "upper bound" for CO_2–CH_4 separation. The different trajectories of enhancement for the low and high pressure cases are the results of Langmuir saturation in zeolite 4A and altered PVAc transport properties as described above. Perhaps most significant is how positively the MMM properties compare to those of cellulose acetate—a commonly used polymer for natural gas separations—as shown in Fig. 7. The properties of the advanced polymer, 6FDA-ODA, are also shown to highlight that further enhancements in separation performance are required for these materials to achieve "upper-bound" status.

5. Conclusions

Poly(vinyl acetate) was used as the polymer matrix to form high zeolite 4A loading MMMs. Mixed CO_2–CH_4 feeds were permeated through these MMMs at 35 °C to assess the viability of these materials for natural gas purification. Although PVAc and zeolite 4A were primarily chosen as inexpensive, well studied model materials, the resulting transport enhancements were quite significant. Plotting the 2 mixed feed cases' permeation properties on Robeson's most current CO_2–CH_4 upper-bound illustrates that the MMMs properties are surprisingly good. Furthermore, most of the values on Robeson's upper-bounds are from low pressure, pure gas permeation experiments. Mixed feed permselectivities of polymers (especially for high p_{CO_2} CO_2–CH_4 feeds) are typically lower than their pure gas counterparts—this further highlights the significance of the properties measured in this work. Overall, it is shown that low performance, low cost polymers, like PVAc, which are typically neglected for gas separation membrane applications, may in fact have a place in real gas separations if filler loadings can be increased further.

Acknowledgements

NSF-STC (CERSP) under agreement CHE-9876674 and Award no. KUS-I1-011-21 made by the King Abdullah University of Science and Technology (KAUST) for this research.

References

[1] C.M. Zimmerman, A. Singh, W.J. Koros, Tailoring mixed matrix composite membranes for gas separations, Journal of Membrane Science 137 (1–2) (1997) 145–154.
[2] M.D. Jia, K.V. Peinemann, R.D. Behling, Molecular-sieving effect of the zeolite-filled silicone-rubber membranes in gas permeation, Journal of Membrane Science 57 (2–3) (1991) 289–296.
[3] H.J.C. Tehennepe, D. Bargeman, M.H.V. Mulder, C.A. Smolders, Zeolite-filled silicone-rubber membranes.1. Membrane preparation and pervaporation results, Journal of Membrane Science 35 (1) (1987) 39–55.
[4] T.S. Chung, L.Y. Jiang, Y. Li, S. Kulprathipanja, Mixed matrix membranes (MMMs) comprising organic polymers with dispersed inorganic fillers for gas separation, Progress in Polymer Science 32 (4) (2007) 483–507.
[5] G. Clarizia, C. Algieria, E. Drioli, Filler–polymer combination: a route to modify gas transport properties of a polymeric membrane, Polymer 45 (16) (2004) 5671–5681.
[6] Y. Li, T.S. Chung, C. Cao, S. Kulprathipanja, The effects of polymer chain rigidification, zeolite pore size and pore blockage on polyethersulfone (pes)-zeolite a mixed matrix membranes, Journal of Membrane Science 260 (1–2) (2005) 45–55.
[7] T.T. Moore, R. Mahajan, D.Q. Vu, W.J. Koros, Hybrid membrane materials comprising organic polymers with rigid dispersed phases, AICHE Journal 50 (2) (2004) 311–321.
[8] A.M.W. Hillock, S.J. Miller, W.J. Koros, Crosslinked mixed matrix membranes for the purification of natural gas: effects of sieve surface modification, Journal of Membrane Science 314 (1–2) (2008) 193–199.
[9] S. Husain, W.J. Koros, Mixed matrix hollow fiber membranes made with modified hssz-13 zeolite in polyetherimide polymer matrix for gas separation, Journal of Membrane Science 288 (1–2) (2007) 195–207.
[10] H.H. Yong, N.C. Park, Y.S. Kang, J. Won, W.N. Kim, Zeolite-filled polyimide membrane containing 2,4,6-triaminopyrimidine, Journal of Membrane Science 188 (2) (2001) 151–163.
[11] J.M. Duval, B. Folkers, M.H.V. Mulder, G. Desgrandchamps, C.A. Smolders, Adsorbent filled membranes for gas separation. 1. Improvement of the gas separation properties of polymeric membranes by incorporation of microporous adsorbents, Journal of Membrane Science 80 (1993) 189–198.
[12] S.B. Tantekin-Ersolmaz, C. Atalay-Orala, M. Tather, A. Erdem-Senatalar, B. Schoeman, J. Sterte, Effect of zeolite particle size on the performance of polymer–zeolite mixed matrix membranes, Journal of Membrane Science 175 (2) (2000) 285–288.
[13] H.T. Wang, B.A. Holmberg, Y.S. Yan, Homogeneous polymer–zeolite nanocomposite membranes by incorporating dispersible template-removed zeolite nanocrystals, Journal of Materials Chemistry 12 (12) (2002) 3640–3643.
[14] M.G. Suer, N. Bac, L. Yilmaz, Gas permeation characteristics of polymer–zeolite mixed matrix membranes, Journal of Membrane Science 91 (1–2) (1994) 77–86.
[15] A.L. Khan, A. Cano-Odena, B. Gutierrez, C. Minguillon, I.F.J. Vankelecom, Hydrogen separation and purification using polysulfone acrylate–zeolite mixed matrix membranes, Journal of Membrane Science 350 (1–2) (2010) 340–346.
[16] K. Diaz, L. Garrido, M. Lopez-Gonzalez, L.F. Del Castillo, E. Riande, Co_2 transport in polysulfone membranes containing zeolitic imidazolate frameworks as determined by permeation and pfg nmr techniques, Macromolecules 43 (1) (2010) 316–325.
[17] D.R. Paul, D.R. Kemp, Diffusion time lag in polymer membranes containing adsorptive fillers, Journal of Polymer Science Part C: Polymer Symposium 41 (1973) 79–93.
[18] W.I. Higuchi, T. Higuchi, Theoretical analysis of diffusional movement through heterogeneous barriers, Journal of the American Pharmaceutical Association 49 (9) (1960) 598–606.
[19] S. Kulprathipanja, Separation of fluids by means of mixed matrix membranes, U.S. P. Office. (1988) 4,740,219.
[20] L.M. Robeson, The upper bound revisited, Journal of Membrane Science 320 (1–2) (2008) 390–400.
[21] W.J. Koros, T.T. Moore, Organic–inorganic hybrid membrane materials for gas separation, in: American Chemical Society (Conference Proceedings), ACS, 2003.
[22] R. Adams, C. Carson, J. Ward, R. Tannenbaum, W. Koros, Metal organic framework mixed matrix membranes for gas separations, Microporous and Mesoporous Materials 131 (1–3) (2010) 13–20.
[23] R. Pal, Permeation models for mixed matrix membranes, Journal of Colloid and Interface Science 317 (1) (2008) 191–198.

[24] A. Erdem-Senatalar, M. Tatlier, S.B. Tantekin-Ersolmaz, Questioning the validity of present models for estimating the performances of zeolite–polymer mixed matrix membranes, in: Chemical Engineering Communications (Conference Proceedings), Taylor & Francis Ltd., 2003.
[25] R. Mahajan, W.J. Koros, Mixed matrix membrane materials with glassy polymers. Part 1, Polymer Engineering and Science 42 (7) (2002) 1420–1431.
[26] R. Mahajan, W.J. Koros, Mixed matrix membrane materials with glassy polymers. Part 2, Polymer Engineering and Science 42 (7) (2002) 1432–1441.
[27] S. Kulprathipanja, Mixed matrix membrane development, in: Advanced Membrane Technology (Conference Proceedings), New York Academy of Sciences, 2003.
[28] W.J. Koros, G.K. Fleming, Membrane-based gas separation, Journal of Membrane Science 83 (1) (1993) 1–80.
[29] R.E. Kesting, A.K. Fritzsche, Polymeric Gas Separation Membranes, John Wiley & Sons, Inc., 1993.
[30] B.D. Bhide, S.A. Stern, Membrane processes for the removal of acid gases from natural-gas. 1. Process configurations and optimization of operating-conditions, Journal of Membrane Science 81 (3) (1993) 209–237.
[31] B.D. Bhide, S.A. Stern, Membrane processes for the removal of acid gases from natural-gas. 2. Effects of operating-conditions, economic-parameters, and membrane-properties, Journal of Membrane Science 81 (3) (1993) 239–252.
[32] S.A. Stern, Polymers for gas separations—the next decade, Journal of Membrane Science 94 (1994) 1–65.
[33] R.W. Baker, K. Lokhandwala, Natural gas processing with membranes: an overview, Industrial and Engineering Chemistry Research 47 (7) (2008) 2109–2121.
[34] T.T. Moore, W.J. Koros, Non-ideal effects in organic–inorganic materials for gas separation membranes, Journal of Molecular Structure 739 (1–3) (2005) 87–98.
[35] W.J. Koros, D.R. Paul, A.A. Rocha, Carbon-dioxide sorption and transport in polycarbonate, Journal of Polymer Science Part B: Polymer Physics 14 (4) (1976) 687–702.
[36] D.R. Paul, W.J. Koros, Effect of partially immobilizing sorption on permeability and diffusion time lag, Journal of Polymer Science Part B-Polymer Physics 14 (4) (1976) 675–685.
[37] R.M. Barrer, Diffusivities in glassy-polymers for the dual mode sorption model, Journal of Membrane Science 18 (1984) 25–35 (MAR).
[38] J. Karger, Measurement of diffusion in zeolites—a never ending challenge? in: International Adsorption Society (Conference Proceedings), 2003, Journal of the International Adsorption Society.
[39] R. Mahajan, R. Burns, M. Schaeffer, W.J. Koros, Challenges in forming successful mixed matrix membranes with rigid polymeric materials Journal of Applied Polymer Science 86 (4) (2002) 881–890.
[40] R. Mahajan, W.J. Koros, Factors controlling successful formation of mixed-matrix gas separation materials, Industrial and Engineering Chemistry Research 39 (8) (2000) 2692–2696.
[41] T.T. Moore, W.J. Koros, Gas sorption in polymers, molecular sieves, and mixed matrix membranes, Journal of Applied Polymer Science 104 (6) (2007) 4053–4059.
[42] D.W. Breck, Zeolite Molecular Sieves, Wiley, New York, 1973.
[43] T.T. Moore, S. Damle, P.J. Williams, W.J. Koros, Characterization of low permeability gas separation membranes and barrier materials; design and operation considerations, Journal of Membrane Science 245 (1–2) (2004) 227–231.
[44] S.G. Croll, Effect of titania pigment on the residual strain, glass-transition and mechanical-properties of a pmma coating, Polymer 20 (11) (1979) 1423–1430.
[45] L.F. Francis, A.V. Mccormick, D.M. Vaessen, J.A. Payne, Development and measurement of stress in polymer coatings, Journal of Materials Science 37 (22) (2002) 4717–4731.
[46] D.R. Kemp, D.R. Paul, Gas sorption in polymer membranes containing adsorptive fillers, Journal of Polymer Science Part B: Polymer Physics 12 (3) (1974) 485–500.
[47] S.S. Kasargod, T.A. Barbari, Permeation breakthrough models for associating and solvating penetrants in a membrane, Industrial and Engineering Chemistry Research 36 (2) (1997) 483–492.
[48] W.J. Koros, D.R. Paul, Design considerations for measurement of gas sorption in polymers by pressure decay, Journal of Polymer Science Part B: Polymer Physics 14 (10) (1976) 1903–1907.
[49] IZASC. Database of zeolite structures (2009). Available from: <http://www.iza-structure.org/databases/>.
[50] J.D. Perry, Formation and characterization of hybrid membranes utilizing high-performance polyimides and carbon molecular sieves, Ph.D. Thesis, Georgia Institute of Technology (2007).